Technical Notes

TECHNICAL NOTES are short manuscripts describing new developments or important results of a preliminary nature. These Notes cannot exceed 6 manuscript pages and 3 figures; a page of text may be substituted for a figure and vice versa. After informal review by the editors, they may be published within a few months of the date of receipt. Style requiremenis are the same as for regular contributions (see inside back cover).

Rectangular Model for Nongray Radiative Transfer

A. L. Crosbie*
University of Missouri-Rolla, Rolla, Mo.
AND
R. Viskanta†
Purdue University, Lafayette, Ind.

Nomenclature

$E_n(\tau)$ = exponential integral, $E_n(\tau) = \int_0^1 \mu^{n-2} \exp(-\tau/\mu)d\mu$
$\mathfrak{F}^+$ = dimensionless flux, $\mathfrak{F}^+$ = radiative flux/σT_2^4
$I_i(\theta)$ = $\frac{15}{\pi^4}\int_{\bar{\nu}_{i-1}/\theta}^{\bar{\nu}_i/\theta} \frac{x^3}{e^x - 1}dx$
$\bar{S}$ = dimensionless heat generation, $\bar{S}$ = heat generation/$\beta\sigma T_2^4$
T = temperature
$\alpha(\nu)$ = spectral dependence of the absorption coefficient, κ_ν
$\beta(T)$ = temperature dependence of the absorption coefficient, κ_ν
θ = dimensionless temperature, $\theta = T/T_2$
ν = frequency
$\bar{\nu}$ = dimensionless frequency, $\bar{\nu} = h\nu/kT_2$ where h is Planck's constant and k is Boltzmann's constant
σ = Stefan-Boltzmann constant
τ = optical depth, $\tau = \int_0^y \beta dy$ where y is the coordinate
τ_o = optical thickness, $\tau_o = \int_0^L \beta dy$ where L is the layer thickness

Subscripts

1,2 = refers to plates 1 and 2

Introduction

In a previous investigation[1] the authors have analyzed the problem of radiative transfer in a plane layer of a nongray absorbing and emitting medium bounded by two black parallel plates maintained at constant temperatures T_1 and T_2. The medium was capable of generating heat, while conductive and convective heat transfer was neglected. The spectral absorption coefficient κ_ν was considered to be of the Milne-Eddington type, i.e., $\kappa_\nu(T) = \alpha(\nu)\beta(T)$, and the function $\alpha(\nu)$ had only values of zero and unity.

It is the purpose of this brief Note to extend the above work by considering a more general function $\alpha(\nu)$. We consider $\alpha(\nu)$ to be defined as

$$\alpha(\nu) = \alpha_i \text{ for } \nu_{i-1} < \nu < \nu_i,\ i = 1, 2, \ldots n \qquad (1)$$

where the limits of the spectrum correspond to $\nu_0 = 0$ and $\nu_n = \infty$. The constant α_i is the magnitude of $\alpha(\nu)$ in the frequency interval between ν_{i-1} and ν_i. The numerical values of α_i can range from zero to unity. Since the spectral dependence of the absorption coefficient is approximated by rectangles, the model is referred to as a rectangular model. In principle, any spectral dependence [form of $\alpha(\nu)$] can be accurately approximated by this model. As in numerical integration, the accuracy of the model is increased by dividing the frequency spectrum into smaller intervals.

Table 1 Models for $\alpha(\bar{\nu})$

Frequency interval	$\alpha(\bar{\nu})$ Model E	$\alpha(\bar{\nu})$ Model F
$0 \le \bar{\nu} < \bar{\nu}_c$	1	α
$\bar{\nu} \ge \bar{\nu}_c$	α	1

Analysis

The conservation of energy equation in dimensionless form for the problem considered can be expressed as[2]

$$\theta^4(\tau)\sum_{i=1}^{n}\alpha_i I_i[\theta(\tau)] = \frac{\bar{S}}{4} + \frac{1}{2}\theta_1^4\sum_{i=1}^{n}\alpha_i I_i(\theta_1)E_2(\alpha_i\tau) + \frac{1}{2}\sum_{i=1}^{n}\alpha_i I_i(1)E_2[\alpha_i(\tau_o - \tau)] + \frac{1}{2}\sum_{i=1}^{n}\int_0^{\tau_o}\theta^4(t)I_i[\theta(t)]\alpha_i^2 E_1(\alpha_i|\tau - t|)dt \qquad (2)$$

In general, when the absorption coefficient has values other than zero and unity, the energy equation for the dimensionless temperature $\theta(\tau)$ results in a nonlinear Fredholm integral equation of the second kind. Because of the nonlinearity, the number of techniques available for solving the equation is limited. The method of successive approximations was chosen for its simplicity and ease of application on a digital computer. The accuracy obtainable by the method is limited only by the size of the computer and the amount of computer time available. Application of the method of successive ap-

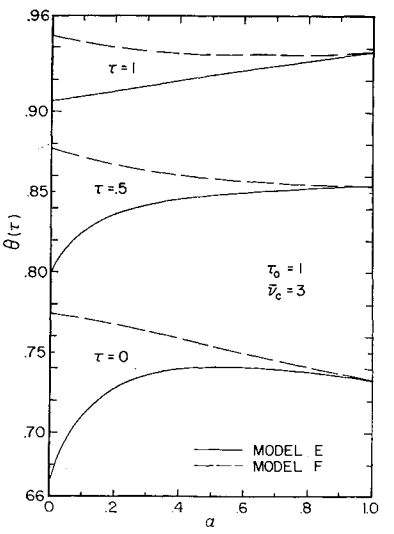

Fig. 1 Effect of α on the temperature distribution for models E and F, $\theta_1 = 0.5$, $\bar{\nu}_c = 3$, $\tau_o = 1$.

Received April 8, 1970; revision received June 5, 1970.
* Assistant Professor, Department of Mechanical and Aerospace Engineering. Member AIAA.
† Professor, School of Mechanical Engineering. Member AIAA.

Table 2 Effect of α on the temperature distribution for model E, $\theta_1 = 0.5$, $\bar{\nu}_c = 3$, $\tau_o = 1$

	$\theta(\tau)$						
τ	$\alpha = 0$	$\alpha = 0.05$	$\alpha = 0.1$	$\alpha = 0.3$	$\alpha = 0.5$	$\alpha = 0.9$	$\alpha = 1.0$
0	0.6683	0.6937	0.7095	0.7357	0.7408	0.7357	0.7334
0.05	0.6878	0.7132	0.7288	0.7540	0.7590	0.7552	0.7534
0.10	0.7030	0.7280	0.7432	0.7656	0.7726	0.7700	0.7685
0.20	0.7296	0.7532	0.7674	0.7900	0.7954	0.7948	0.7939
0.30	0.7536	0.7753	0.7882	0.8092	0.8148	0.8162	0.8158
0.40	0.7762	0.7956	0.8071	0.8263	0.8323	0.8354	0.8355
0.50	0.7977	0.8146	0.8247	0.8421	0.8484	0.8532	0.8537
0.60	0.8187	0.8328	0.8413	0.8570	0.8635	0.8699	0.8708
0.70	0.8393	0.8506	0.8574	0.8712	0.8781	0.8858	0.8872
0.80	0.8600	0.8682	0.8734	0.8852	0.8922	0.9014	0.9031
0.90	0.8815	0.8865	0.8899	0.8994	0.9066	0.9171	0.9191
0.95	0.8931	0.8964	0.8988	0.9071	0.9143	0.9254	0.9276
1.00	0.9072	0.9086	0.9098	0.9164	0.9235	0.9353	0.9377
$\mathfrak{F}^+ =$	0.7860	0.7604	0.7376	0.6644	0.6101	0.5336	0.5188

proximations to Eq. (2) yields

$$\theta_{k+1}^4(\tau)\sum_{i=1}^{n}\alpha_i I_i[\theta_k(\tau)] = \frac{\bar{S}}{4} + \frac{1}{2}\theta_1^4\sum_{i=1}^{n}\alpha_i I_i(\theta_1)E_2(\alpha_i\tau) + \frac{1}{2}\sum_{i=1}^{n}\alpha_i I_i(1)E_2[\alpha_i(\tau_o - \tau)] + \frac{1}{2}\sum_{i=1}^{n}\int_0^{\tau_o}\theta_k^4(t)I_i[\theta_k(t)]\alpha_i^2 E_1(\alpha_i|\tau - t|)dt \qquad (3)$$

$$k = 0, 1, 2, \ldots$$

where $\theta_0(\tau) = 1$ is the zeroth approximation. The number of iterations and thus the computer time required increases as the optical thickness is increased.

Once the temperature distribution is known, the local radiative flux can be calculated. Introducing the dimensionless quantities, the radiative flux becomes[2]

$$\mathfrak{F}^+ = 2\theta_1^4\sum_{i=1}^{n}\alpha_i I_i(\theta_1)E_3(\alpha_i\tau) - 2\sum_{i=1}^{n}\alpha_i I_i(1) \times E_3[\alpha_i(\tau_o - \tau)] + 2\sum_{i=1}^{n}\int_0^{\tau_o}\theta^4(t)I_i \times [\theta(t)]\,\mathrm{sign}(\tau - t)\alpha_i E_2(\alpha_i|\tau - t|)dt \qquad (4)$$

Obviously, there are many interesting models that could be considered. Unlike the linear situation,[1] the nonlinear integral equation must be solved for each variation in the spectral absorption coefficient. Since the numerical solution of an integral equation is quite time consuming, the number of models studied in this brief is restricted to the example discussed below.

Example

As an illustration, two simple models for the absorption coefficient are used in the study. The models are designated by alphabetic symbols, and the characteristics of each model are presented in Table 1. Models E and F are equivalent to the linear models A and B of Ref. 1, respectively, when $\alpha = 0$. Although the models consist of only two steps, more complex models can be treated in a similar manner.

The "exact" numerical solutions of energy equation (3) have been obtained for these two nongray absorption coefficients. For each model, there are five independent parameters: τ_o, $\bar{\nu}_c$, α, θ_1, $\bar{S}$. Since the effect of τ_o, $\bar{\nu}_c$, and θ_1 have been investigated for the linear situation ($\alpha = 0$), these parameters are assigned the following representative values throughout the remainder of the discussion: $\tau_o = 1$, $\bar{\nu}_c = 3$, $\theta_1 = 0.5$, and $\bar{S} = 0$ (radiative equilibrium). Approximately 39% of the blackbody radiation comes from the frequency interval $0 \leq \bar{\nu} \leq 3$, while 61% comes from the frequency interval $\bar{\nu} \geq 3$.

The effect of the parameter α on the temperature distribution is presented in Fig. 1 and Tables 2 and 3. The largest variation in the temperature with α occurs at $\tau = 0$ for both models, while the temperature at $\tau = 1$ is affected the least. For model F, the temperature at $\tau = 0$ appears to be bounded between the gray case ($\alpha = 1$) and results for model B ($\alpha = 0$). In fact, the variation of $\theta(0)$ with α is almost linear. However, for model E the temperature at $\tau = 0$ has a value

Table 3 Effect of α on the temperature distribution for model F, $\theta_1 = 0.5$, $\bar{\nu}_c = 3$, $\tau_o = 1$

	$\theta(\tau)$						
τ	$\alpha = 0$	$\alpha = 0.1$	$\alpha = 0.4$	$\alpha = 0.5$	$\alpha = 0.6$	$\alpha = 0.8$	$\alpha = 1$
0	0.7744	0.7712	0.7588	0.7544	0.7500	0.7414	0.7334
0.05	0.7921	0.7879	0.7752	0.7712	0.7673	0.7600	0.7534
0.10	0.8053	0.8004	0.7878	0.7841	0.7806	0.7742	0.7685
0.20	0.8272	0.8114	0.8091	0.8059	0.8030	0.7981	0.7939
0.30	0.8459	0.8395	0.8277	0.8250	0.8226	0.8188	0.8158
0.40	0.8627	0.8558	0.8446	0.8423	0.8404	0.8376	0.8355
0.50	0.8781	0.8710	0.8604	0.8585	0.8571	0.8550	0.8537
0.60	0.8925	0.8853	0.8754	0.8739	0.8728	0.8715	0.8709
0.70	0.9062	0.8990	0.8900	0.8888	0.8880	0.8872	0.8872
0.80	0.9195	0.9125	0.9043	0.9034	0.9029	0.9027	0.9031
0.90	0.9328	0.9263	0.9190	0.9183	0.9180	0.9183	0.9191
0.95	0.9399	0.9336	0.9268	0.9263	0.9261	0.9266	0.9276
1.00	0.9483	0.9426	0.9364	0.9359	0.9359	0.9365	0.9377
$\mathfrak{F}^+ =$	0.6703	0.6427	0.5846	0.5702	0.5576	0.5362	0.5188

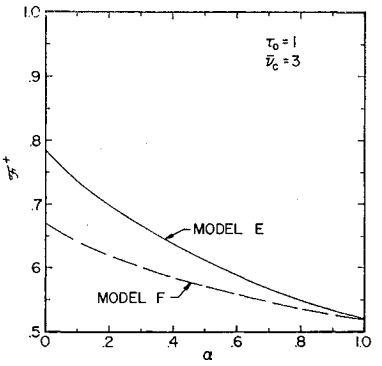

Fig. 2 Effect of α on the radiative flux for models E and F, $\theta_1 = 0.5$, $\bar{\nu}_c = 3$, $\tau_o = 1$.

greater than the gray case for $\alpha \geq 0.26$. The maximum value of the temperature [$\theta(0) \simeq 0.741$] occurs near $\alpha = 0.5$. The situation is reversed at $\tau = 1$. The temperature for model F has a minimum near $\alpha = 0.5$, and $\theta(\tau_o)$ for model E is almost linear with α. For any given value of $\alpha < 1$ and any τ, the temperature for model F is always greater than that for model E.

The numerical values for $\mathfrak{F}^+$ are given in Tables 2 and 3 as well as illustrated graphically in Fig. 2. For all values of $\alpha \geq 0$, the energy transferred between the plates is greatest for model E. As expected, for both models the radiative flux is a monotonically decreasing function of α and reduces to the gray result for $\alpha = 1$.

References

[1] Crosbie, A. L. and Viskanta, R., "The Exact Solution to a Simple Nongray Radiative Transfer Problem," *Journal of Quantitative Spectroscopy and Radiative Transfer*, Vol. 9, 1969, pp. 553–568.

[2] Crosbie, A. L., "Radiation Heat Transfer in a Nongray Planar Medium," Ph.D. thesis, 1969, Purdue University.

An Extension to Existing Methods of Determining Refractive Indices from Axisymmetric Interferograms

ROBERT SOUTH*
The Gas Council, Watson House, London, England

Nomenclature

N = refractive index in disturbance
N_o = refractive index in reference field
r = radius $= (x^2 + y^2)^{1/2}$
R_0 = radius of axisymmetric disturbance
S = fringe shift
x,y,z = rectangular coordinates, with x in the direction of the light beam and z the axis of symmetry
λ = vacuum wavelength of light

1. Introduction

IT is often required to determine the density or temperature in an axisymmetric system, such as the flow field around a missile, or the mass transfer field in a jet. For obvious reasons optical methods are particularly suitable for making measurements of this sort and interferometry, in particular, has found wide application.

Received May 12, 1970; revision received June 29, 1970. The author would like to thank J. P. Price for advice and assistance on the foregoing mathematics and also the Gas Council and the City University for permission to publish this paper.

* Research Physicist, Combustion Research Group.

Various methods have been evolved for analyzing axisymmetric interferograms, and these are generally satisfactory when the fringe shift distribution is a simple function of lateral distance. However, when the fringe shift distribution is relatively complex, as is the case for interferograms of axisymmetric laminar diffusion flames, the existing methods are not entirely satisfactory. The foregoing problem has led the author to develop a method of analyzing interferograms of axisymmetric laminar flames, and the method developed would appear to be altogether more generally applicable than existing methods.

2. Existing Methods

A fringe shift results from the difference in optical path of two light beams, one of which passes through the refractive index disturbance and the other through a reference refractive index field. If the disturbance shows axial symmetry about, say, the z axis, the fringe shift, which is the difference in wavelengths of the optical paths of the two light beams, is given by

$$S(y) = \frac{1}{\lambda}\int_{x_1}^{x_2} [N(x) - N_0]dx \tag{1}$$

where x is in the direction of the light beam. In polar coordinates Eq. (1) becomes

$$S(y) = \frac{2}{\lambda}\int_{y}^{R_0} [N(r) - N_0]rdr/(r^2 - y^2)^{1/2} \tag{2}$$

where, Fig. 1, $r = (x^2 + y^2)^{1/2}$, and R_0 is the radius of the disturbance, i.e., where $N(r) = N_0$.

If the functions are suitably well behaved, then by Abel's transformation Eq. (2) becomes

$$N(r) - N_0 = -\frac{\lambda}{\pi r}\frac{d}{dr}\int_{r}^{R_0} \frac{S(y)ydy}{(y^2 - r^2)^{1/2}} \tag{3}$$

Freeman and Katz[1] have used Eq. (3) for analyzing radiance profiles in plasma discharges for those cases where the data can be fitted by least squares to a simple functional form.

Bradley[2] used a similar approach in which the observed fringe shift distribution is represented in the unit interval by a cubic and the coefficients are determined by a least squares fit of the observed fringe shift values.

However, the solutions discussed above and the forerunners of these[3–5] are not particularly suitable for those cases, such as the analysis of axisymmetric flames, where the observed fringe shift distribution is a relatively complex function of lateral distance.

3. A More General Approach

We now propose an extension to the existing approaches that is suitable for cases where the complete observed lateral fringe shift distribution cannot adequately be represented within experimental error of the data by a single curve of sufficiently low order. To be acceptable, a representation should be reasonably low-ordered, correlate the data to within experimental error, and introduce no unwarranted inflection points.

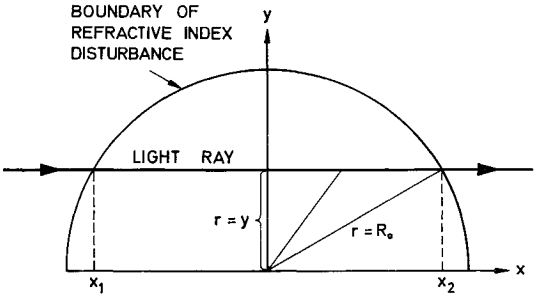

Fig. 1 Axisymmetric refractive index disturbance traversed by a light beam.